

CHAPTER 40

LONG WAVES GENERATED BY COMPLEX BOTTOM MOTIONS

J. L. Hammack
Associate Professor of Civil Engineering
University of California, Berkeley, U.S.A.

and

F. Raichlen
Professor of Civil Engineering
California Institute of Technology, Pasadena, U.S.A.

1. Introduction

Studies of tsunami generation often employ simple models of the sea floor dislocations to permit tractable analytical solutions. Although these solutions provide basic insight into the generation process, they are incapable of producing explicit results for prototype events where both the spatial and temporal distributions of the sea floor dislocation may be quite complicated. Herein we exploit the apparent linearity of the generation process and demonstrate both the use and validity of the superposition principle to construct solutions for complex bed motions. Analytical and experimental results are presented for a monopolar dislocation (block upthrust or downthrow) with a complex time-displacement history. The time history used in the computations is obtained from an integrated accelerogram recorded at Pacoima Dam, near Los Angeles, during the earthquake of February 9, 1971. A complex spatial deformation is not used in order to enable experimental verification of the analytical results. This is unfortunate since it appears that the details of the time-displacement history are not important for prototype phenomena where the motion may be considered instantaneous. However, it is important to note that the analysis treats both space and time variations in an identical manner; hence, confirmation of this approach for complex time variations strongly suggests analogous behavior for complex spatial variations.

Finally, we examine and compare several alternative time-displacement histories for the mean motion. It is shown that the results for each mean motion can be unified by introducing a velocity as a descriptive parameter which is based on the kinetic energy input of the moving bottom to the overlying fluid.

2. Time-Displacement History

To define a complicated time-displacement history with relevance to earthquake-induced ground motions, we have chosen an accelerogram for the vertical component of motion recorded at Pacoima Dam (near Los Angeles) during the earthquake of February 9, 1971. The accelerogram

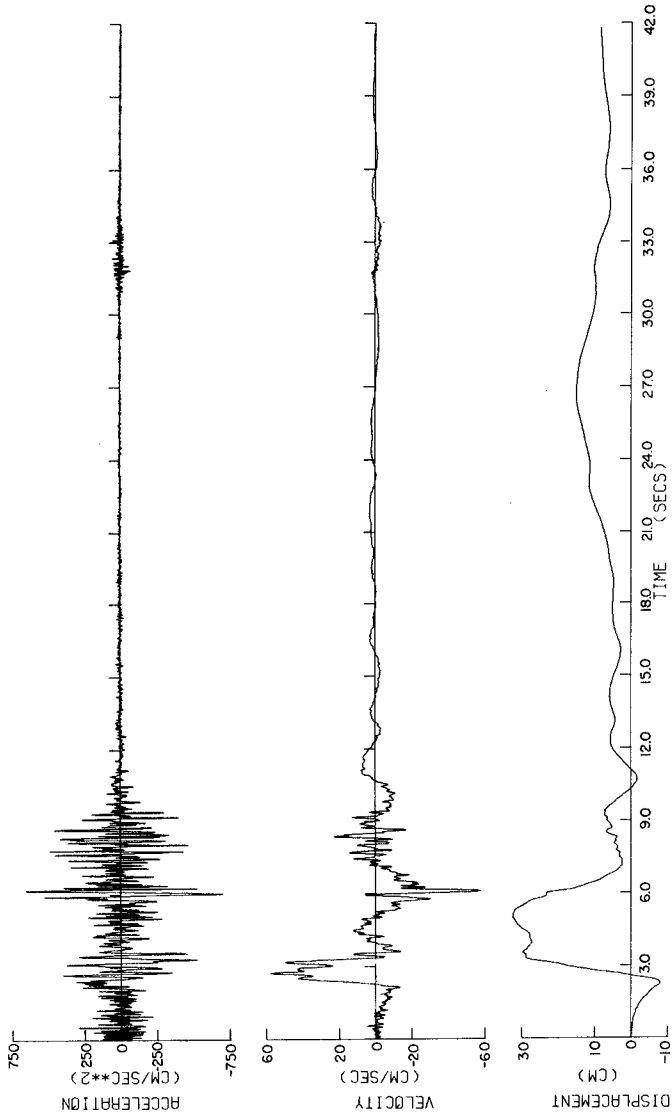


Figure 1. Vertical component of ground acceleration recorded 2/9/71 0600 PST Pacoima Dam, California, with integrated velocity and ground displacement.

shown in Figure 1 may be integrated numerically using appropriate precautions (e.g., see Nigam and Jennings, 1968), to yield a time history of the vertical ground displacement. Results of the integration process for the "smoothed" velocity history and the corresponding ground displacement history are shown below the accelerogram in Figure 1.

An analytical representation of the algebraically complex time-displacement history of Figure 1 over a finite record interval, $0 \leq t \leq T$, may be constructed using a Fourier series of the form:

$$\zeta(t) = C_0 + \sum_{n=1}^N C_n \sin(K_n t + \beta_n). \quad (1)$$

In (1) C_n are the amplitudes of the Fourier components with C_0 representing the mean (permanent) ground displacement, K_n are the component wave frequencies, and β_n are the component phase angles. The accuracy of (1) in representing the integrated displacement of Figure 1 is determined by the number of components N retained in the Fourier sum. Results of computations with $N = 18$ are illustrated in Figure 2; this truncated sum will be adopted in the subsequent analysis.

It should be emphasized that both the instrument characteristics and the numerical integration techniques used to obtain ground displacements from acceleration measurements necessarily distort (filter) information in long period components. In particular, the mean (and permanent) displacement of the integrated motion shown in Figure 1 (and, of course, its Fourier representation in Figure 2) is not expected to accurately model the actual permanent deformation. To compensate for this distortion, we may again exploit the superposition principle and add a nonsinusoidal component to the Fourier series representation of (1). As an example of this approach, consider the ramp motion in time of the form:

$$\zeta_r(t) = \zeta_0 t/T \quad (2)$$

during the time interval $0 \leq t \leq T$; other choices for the mean motion are discussed and compared in section 5. In practice, the sum of the mean component resulting from the Fourier synthesis, C_0 , and the additional component ζ_0 from (2) should be chosen to equal the actual permanent ground offset. Hence, a general representation for a complicated time-displacement history becomes:

$$\zeta(t) = C_0 + \zeta_0 t/T + \sum_{n=1}^N C_n \sin(K_n t + \beta_n). \quad (3)$$

3. Solutions of the Water Wave Problem

Consider a two-dimensional (x,y) and incompressible ocean of uniform depth h initially in equilibrium with the earth's gravitational field g which acts in the negative y direction. At time $t = 0$ a section of the

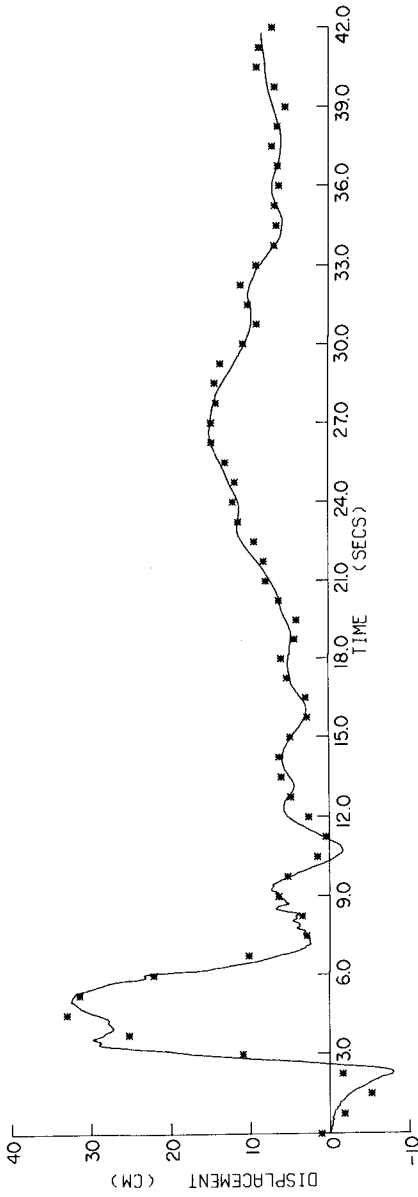


Figure 2. Vertical ground displacement (—) and Fourier synthesis (*) using eighteen components.

sea floor begins to deform vertically with a time and spatial variation given by $\zeta(x,t)$. We seek the inviscid, irrotational, and barotropic deviations $\eta(x,t)$ of the ocean free surface from its equilibrium position. With the coordinate system at the equilibrium position of the free surface, the linearized description of motion in terms of a velocity potential $\phi = \phi(x,y,t)$ is:

$$\phi_{xx}(x,y,t) + \phi_{yy}(x,y,t) = 0 \tag{4}$$

$$\phi_y(x,-h,t) = \zeta_t(x,t) \tag{5}$$

$$\phi_y(x,0,t) = \eta_t(x,t) \tag{6}$$

$$\phi_t(x,0,t) = -g\eta(x,t) \tag{7}$$

where subscripted variables indicate partial differentiation. It is convenient to eliminate $\eta(x,t)$ in (6) and (7) by combining to yield a single condition for the velocity potential:

$$\phi_{tt}(x,0,t) + g\phi_y(x,0,t) = 0 \tag{8}$$

Using the Laplace transform in t and the Fourier transform in x , equations (4), (5) and (8) become:

$$\bar{\phi}_{yy}(k,y,s) - k^2\bar{\phi}(k,y,s) = 0 \tag{9}$$

$$\bar{\phi}_y(k,-h,s) = s\bar{\zeta}(k,s) \tag{10}$$

$$\bar{\phi}_y(k,0,s) + \frac{s^2}{g}\bar{\phi}(k,0,s) = 0 \tag{11}$$

where the overbar of a function $f(x,t)$ indicates:

$$\bar{f}(k,s) = \int_{-\infty}^{\infty} dx \int_{-\infty}^{\infty} e^{ikx} e^{-st} f(x,t) dt. \tag{12}$$

Solving (9), (10), and (11) for $\bar{\phi}(k,y,s)$ and noting from (7) that

$$\bar{\eta}(k,s) = -(s/g)\bar{\phi}(k,0,s) \tag{13}$$

we find:

$$\bar{\eta}(k,s) = s^2 \bar{\zeta}(k,s) / (s^2 + \omega^2) \cosh kh \tag{14}$$

where $\omega^2 = gk \tanh kh$. Inverting the Laplace and Fourier transforms yields:

$$\eta(x,t) = \frac{1}{2\pi} \int_{-\infty}^{\infty} \left\{ \lim_{\Gamma \rightarrow \infty} \frac{1}{2\pi i} \int_{\mu-i\Gamma}^{\mu+i\Gamma} \frac{s^2 e^{-ikx} e^{st}}{(s^2 + \omega^2) \cosh kh} \bar{\zeta}(k,s) ds \right\} dk \tag{15}$$

where the complex inversion integral for the Laplace transform has been used. In (15) ω is the wave frequency ($\omega = is$) and k is the wavenumber. Explicit results for specific deformations of the sea floor $\zeta(x,t)$ will be developed now.

3.1 Solution for a single Fourier component

Consider a block section of the sea floor of length $2b$ whose time-displacement history corresponds to a single Fourier component of (1). With the coordinate system centered above the block section, we have

$$\zeta_n(x,t) = C_n H(b^2 - x^2) [\sin(K_n T + \beta_n) H(T - t) + \sin(K_n t + \beta_n) H(t - T)] \quad (16)$$

where $H(\cdot)$ is the Heaviside step function. Finding the transform of (16), substituting into (15), performing the integration around the Bromwich contour, taking only the real part of the resulting integral, and noting that the integrand is an even function of k , we find:

$$\eta_n(x,t) = \frac{2C_n}{\pi} \int_0^\infty \frac{\cos kx \sin kb}{k \cosh kh} \left\{ A+B - H(t-T) [C+D+E] \right\} dk \quad (17)$$

where

$$A = \sin \beta_n [(\omega^2 \sin \omega t - K_n^2 \sin K_n t)/(\omega^2 - K_n^2)] \quad (18)$$

$$B = K_n \cos \beta_n [(\omega \sin \omega t - K_n \sin K_n t)/(\omega^2 - K_n^2)] \quad (19)$$

$$C = \sin(K_n T + \beta_n) \left\{ [\omega^2 \cos \omega(t-T) - K_n^2 \cos K_n(t-T)]/(\omega^2 - K_n^2) \right\} \quad (20)$$

$$D = K_n \cos(K_n T + \beta_n) \left\{ [\omega \sin \omega(t-T) - K_n \sin K_n(t-T)]/(\omega^2 - K_n^2) \right\} \quad (21)$$

$$E = -\sin(K_n T + \beta_n) \cos \omega(t-T). \quad (22)$$

The final integration over wavenumber k in (17) is obtained by numerical quadratures.

3.2 Solution for ramp mean motion

The ramp time-displacement history of (2) for the block deformation is described by

$$\zeta(x,t) = \zeta_0 H(b^2 - x^2) [tH(T - t)/T + H(t - T)]. \quad (23)$$

Following the same procedure outline in section 3.1, we obtain (again after considerable algebra) the water surface motion η_r due to the ramp

$$\eta_r(x,t) = \frac{2\zeta_0}{\pi} \int_0^\infty \frac{\cos kx \sin kb}{k \cosh kh} \left(\frac{1}{\omega T} \right) [\sin \omega t - H(t - T) \sin \omega(t - T)] dk. \quad (24)$$

Again, the final integration over wavenumber k must be evaluated numerically.

4. Comparison of Theory and Experiment

As noted earlier, the simple block deformation of the sea floor was chosen to enable experimental verification of the analytical model developed for complicated time-displacement histories. The experimental facility used in these tests has been described in detail by Hammack (1972, 1973). Basically, the wave-maker consists of a rectangular piston in the bottom of a wave tank (and spanning its width) whose motion is controlled by an electro-hydraulic-servo system. The servo system converts a time-voltage command signal into a proportional vertical displacement of the piston. For the experiments reported herein, the piston length in the direction of wave motion is $b = 61$ cm while the quiescent water depth above the piston is $h = 10$ cm. Before presenting results of the tests, we describe the motivation for choosing other experimental scales.

A "global" time scale for the forcing of the overlying ocean by the sea floor is the period T . The appropriate time scale for the gravitational response of the long barotropic wave modes is $b/(gh)^{1/2}$ which corresponds to the time required for waves to escape the generation region. For prototypical earthquakes the ratio of the forcing and response time scales, $\tau = T(gh)^{1/2}/b$, termed the time-size ratio, is small so that details of the time-displacement history generally are not important. However, our interests herein require that the details of the temporal motion have a significant impact on the generated wave structure. Hence, the period T for the experimental tests must be scaled so that τ exceeds unity; in fact, for the experiments a period $T = 4$ secs was chosen which yields $\tau = 6.5$. Previous experiments by Hammack (1973) also indicate that the generation process for prototypical tsunamis is linear and that nonlinearity remains insignificant for vertical displacements which do not exceed about 20% of the overlying ocean depth. This criterion is adhered to in the experiments by restricting the instantaneous displacement of the piston to less than 2 cm.

In the first test we examine experimental and theoretical results for the time-displacement history shown in Figure 2 using experimental parameters $T = 4$ secs and a chosen permanent (mean) displacement of $C_0 = 0.38$ cm, with the amplitudes C_n and frequencies K_n of the eighteen Fourier components used in Figure 2 scaled appropriately. (In Figure 2 the corresponding parameters of the actual ground displacement are $T = 40$ secs and $C_0 = 7.63$ cm.) The scaled Fourier components are then summed and the result is converted to an analogue (time-voltage) signal which is used to command the wavemaker. The resulting wave motion at the leading edge of the piston ($x = b$) is measured, and the results are shown in Figure 3. Theoretical results at $x = b$ are evaluated for each of the eighteen (scaled) Fourier components according to (17) and summed to yield

$$\eta(b,t) = C_0 + \sum_{n=1}^{18} \eta_n(b,t); \quad (25)$$

the results also are shown in Figure 3. The excellent agreement between the predicted and measured data is self-evident.

Similar results are shown in Figure 4 where a ramp mean motion with an amplitude of $\zeta_0 = 1.33$ cm is added to the Fourier synthesis of Figure 2. The total permanent displacement of the piston is $\zeta_0' = C_0 + \zeta_0 = 1.71$ cm which has been used to normalize the measured and theoretical wave amplitudes. The theoretical result is equivalent to (25) with an added component for the ramp computed from (24). Again, the agreement between measured and computed data is excellent with the wave structure clearly showing the added volume (mass) resulting from the enhanced mean displacement.

5. A Comment on Mean Motions

In previous studies (Hammack, 1972, 1973) two additional models for the mean displacement of a block section of the sea floor have been examined. These time histories are:

- a. exponential: $\zeta_e(t) = \zeta_0 [1 - \exp(-1.1t/T_e)]$
- b. half-sine: $\zeta_s(t) = \zeta_0 [(1 - \cos \pi t/T_s)H(T_s - t)/2 + H(t - T_s)]$

and we repeat for completeness the mean motion introduced here:

- c. ramp: $\zeta_r(t) = \zeta_0 [tH(T_r - t)/T_r + H(t - T_r)]$.

The three mean motions listed above span a wide range of displacement characteristics. We note that the choice of characteristic time scales T_e , T_s and T_r are, in fact, arbitrary to a certain extent even though "natural" choices are apparent. (This flexibility is most obvious for the exponential motion where T_e was chosen for experimental convenience to represent the time for two-thirds of the displacement to occur.) It has been found that the properties of waves generated by these motions correlated strongly with the time-size ratio τ based on these time scales. For example, the maximum wave amplitude, say η_0 , occurring at $x = b$ when normalized by the permanent displacement ζ_0 exhibits a simple and similar functional dependence on τ for each bed motion. With the size scale b/h of the dislocation fixed and for $\tau \ll 1$, the normalized amplitude, η_0/ζ_0 , reaches a maximum value of one-half for all size scales exceeding unity. Bed motions with $\tau \ll 1$ are termed impulsive. For τ very large, termed creeping generation, η_0/ζ_0 decreases at a rate which is inversely proportional to τ . The constant of proportionality for creeping generation varies with the specific choice of the characteristic time scale for the mean motion. Since it is unlikely that any of these mean motion models is "correct" from a geophysical point of view, there is a need to seek a unification of results by generalizing the concept of characteristic time scale. One generalization which closely

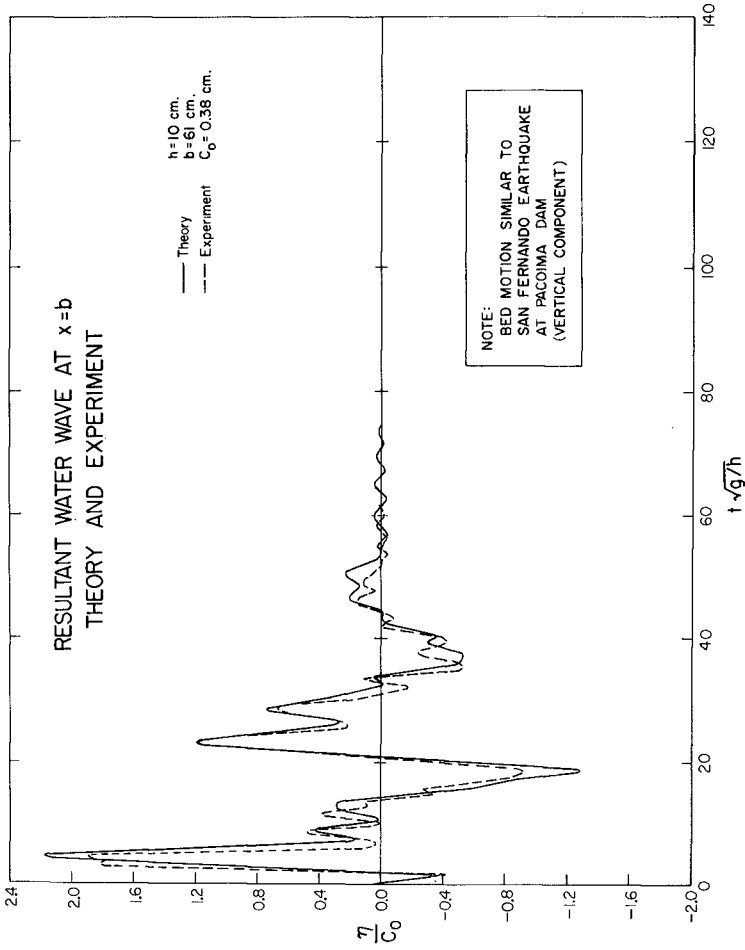


Figure 3. Theoretical (—) and experimental (- - -) wave records at $x = b$.

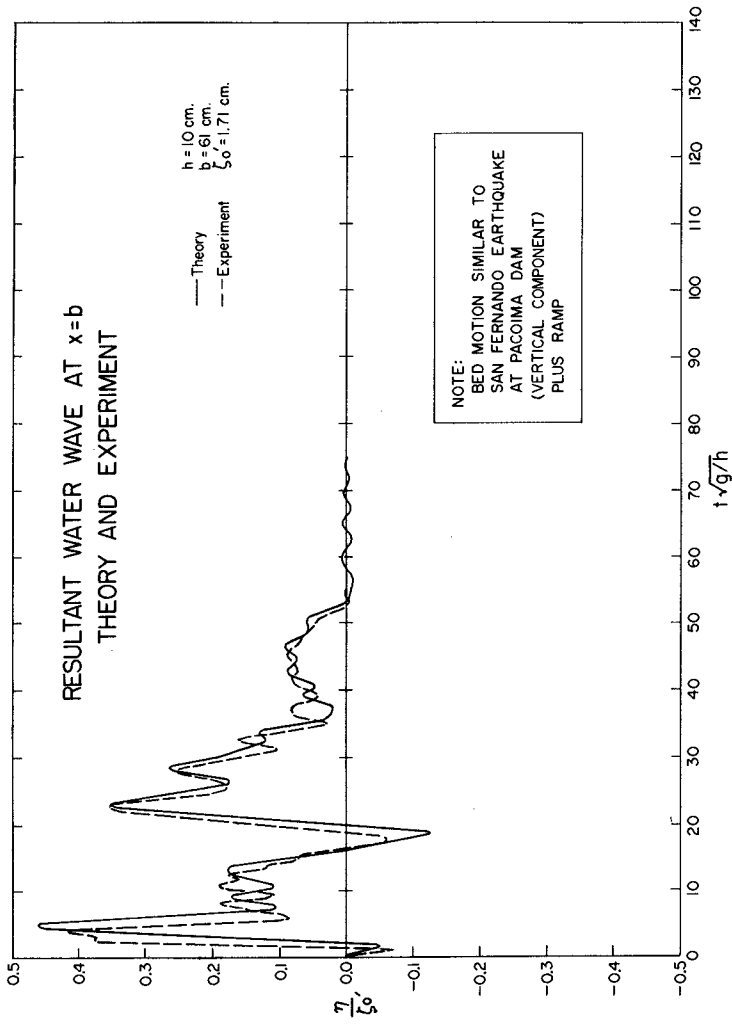


Figure 4. Theoretical (—) and experimental (- - -) wave records at $x = b$ with ramp mean motion.

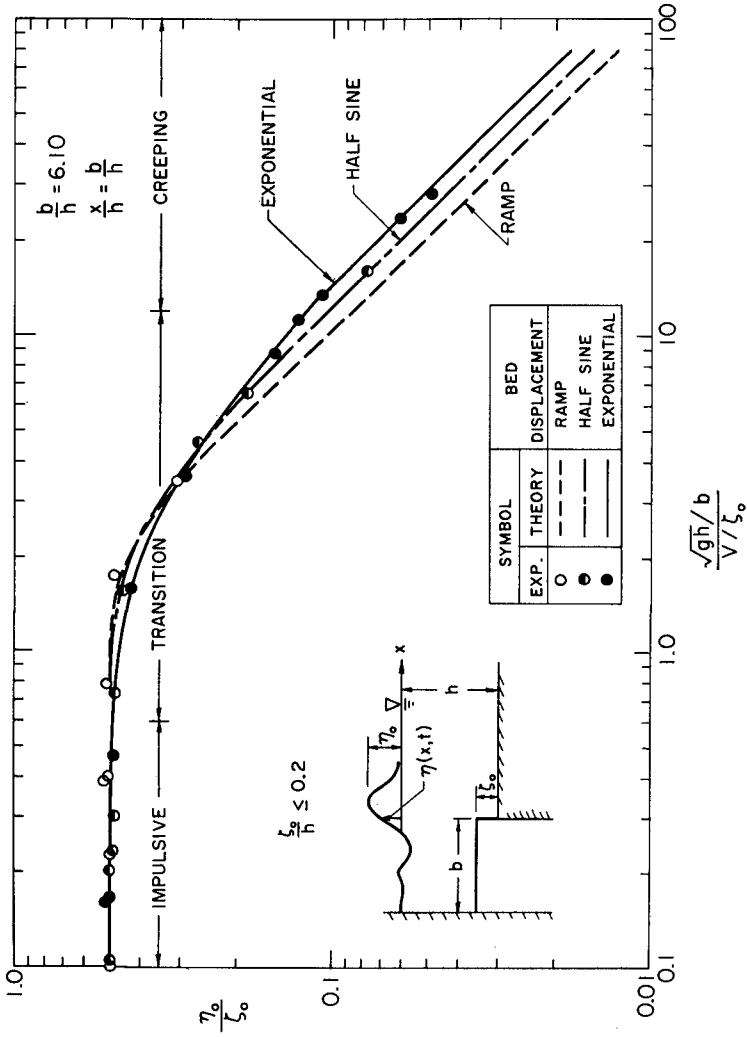


Figure 5. Theoretical and experimental variation of normalized wave amplitude at $x = b$ with generalized time-size ratio for three mean motions.

produces the desired unification is the following. Consider a velocity V , where V^2 is the kinetic energy imparted to the fluid by the sea floor divided by one-half the total mass of fluid displaced during bed motion ($\frac{1}{2} \rho b \zeta_0$); then V is given by:

$$V = \frac{1}{\zeta} \int_0^{\zeta_0} \zeta_t^2 d\zeta \quad (26)$$

and a corresponding time scale $T = \zeta_0/V$. In terms of this time scale the time-size ratio becomes

$$\tau^* = T(gh)^{1/2}/b = \zeta_0(gh)^{1/2}/bV \quad (27)$$

The variation of η_0/ζ_0 at $x = b$ for $b/h = 6.1$ with τ^* is shown in Figure 5 for each of the mean motions; both theoretical and experimental results are presented. For all of the experimental data we have taken $\zeta_0/h < 0.2$ to avoid significant nonlinear effects. The collapse of results for such a wide range of mean motion characteristics shown in Figure 5 is good although a small spread still exists.

6. Conclusions

We have demonstrated both the application and validity of a strategy which employs multiple uses of the superposition principle to develop theoretical solutions for waves generated by sea floor motions with complicated time-displacement histories. Although a more useful test for prototypical phenomena would utilize complicated spatial distributions for the sea floor dislocation, the tests herein were restricted to simple block dislocations due to experimental limitations. However, it is emphasized that the solution method does not distinguish between space and time, and the validity established herein strongly suggests that the methods could be extended to complicated spatial deformations. Finally, we have demonstrated that wave properties (in particular the maximum amplitude of waves escaping the generation region) for a wide range of mean motion characteristics may be (almost) collapsed into a single functional relationship in terms of a time-size ratio based on an average vertical velocity of the sea floor obtained from energy considerations.

7. Acknowledgments

The authors gratefully acknowledge the support of the National Science Foundation under Grant AEN 72-03587-A02 at the California Institute of Technology and the Office of Naval Research under contract N00014-78-C-0889 at the University of California. One author (JLH) would also like to thank the La Jolla Institute, Center for Studies of Nonlinear Dynamics, where portions of this study were completed.

8. References

Hammack, J. L., "Tsunamis: A Model of Their Generation and Propagation," *Report KH-R-28*, W. M. Keck Laboratory of Hydraulics and Water Resources, California Institute of Technology, Pasadena, 1972.

Hammack, J. L., "A Note on Tsunamis: Their Generation and Propagation in an Ocean of Uniform Depth," *Journal of Fluid Mechanics*, Vol. 60, No. 4, 1973, pp. 769-800.

Nigam, N. C., and Jennings, P. C., "Digital Calculation of Response Spectra from Strong-motion Earthquake Records, Earthquake Engineering Research Laboratory Report, California Institute of Technology, Pasadena, 1968.